

Conference Paper

Characteristics and Sensing Properties of the $\text{La}_{1-x}\text{Nd}_x\text{Co}_{0.3}\text{Fe}_{0.7}\text{O}_3$ System for CO Gas Sensors

J.C. Ding, Z.P. Wu, H.Y. Li, Z.X. Cai, X.X. Wang, and X. Guo

Laboratory of Solid State Ionics, School of Materials Science and Engineering, Huazhong University of Science and Technology, Wuhan 430074, P. R. China

Abstract

A series of nanostructured $\text{La}_{1-x}\text{Nd}_x\text{Co}_{0.3}\text{Fe}_{0.7}\text{O}_3$ perovskite-type (x ranging from 0 to 1) were prepared using the co-precipitation method. CO gas sensing properties of $\text{La}_{1-x}\text{Nd}_x\text{Co}_{0.3}\text{Fe}_{0.7}\text{O}_3$ sensors were performed. $\text{La}_{0.7}\text{Nd}_{0.3}\text{Co}_{0.3}\text{Fe}_{0.7}\text{O}_3$ sensor showed the highest response at 250 °C ($S=52.8$).

Keywords: $\text{La}_{1-x}\text{Nd}_x\text{Co}_{0.3}\text{Fe}_{0.7}\text{O}_3$, nanoparticles, CO sensor, $\text{La}_{0.7}\text{Nd}_{0.3}\text{Co}_{0.3}\text{Fe}_{0.7}\text{O}_3$

Corresponding Author: X. Guo;
email: xguo@hust.edu.cn

Received: 9 September 2016
Accepted: 19 September 2016
Published: 12 October 2016

Publishing services provided
by Knowledge E

© J.C. Ding et al. This article is distributed under the terms of the [Creative Commons Attribution License](#), which permits unrestricted use and redistribution provided that the original author and source are credited.

Selection and Peer-review under the responsibility of the ASRTU Conference Committee.

1. Introduction

Carbon monoxide (CO) is colorless, odorless and yet highly toxic gas; it can attack hemoglobin from the blood, preventing the supply of needed oxygen to different parts of human body [1]. Sensors for detecting CO gas have been widely used in many areas, for example, the control of industrial wastes and vehicle emissions, the monitoring of indoor atmosphere and coal mine explosion [2].

Several substituted rare-earth-transition-metal oxides of the perovskite structure (ABO_3) have been used as CO sensors. Among these oxides, LaCoO_3 and LaFeO_3 exhibit excellent CO sensing performance. In our previous work, the characteristics and sensing properties of the $\text{LaCo}_{1-x}\text{Fe}_x\text{O}_3$ system for CO gas sensors have been studied and the $\text{LaCo}_{0.3}\text{Fe}_{0.7}\text{O}_3$ one demonstrated maximal response.

In addition, NdMO_3 ($M = \text{Co}, \text{Fe}$, etc.) exhibits good ability in CO sensing or CO catalytic oxidation. Among them, NdCoO_3 is an excellent sensing material with high sensitivity towards the CO [3-4]. It has been studied for CO sensing and exhibits excellent performances; for example, NdCoO_3 thin film showed a good response (about 15%) for CO concentration until 0.1% and the optimal working temperature was found to be around 300 °C [5]. On the other hand, NdFeO_3 was reported to have good gas-sensing properties for CO. For examples, the NdFeO_3 sensor showed a response of 1215% to 0.03% CO gas at 170°C [6]. In addition, some mixed solution compounds, such as $\text{NdFe}_{1-x}\text{Co}_x\text{O}_3$ [6] and $\text{La}_{1-x}\text{Nd}_x\text{FeO}_3$ [7], have been prepared and their structural, electrical, and gas sensing properties have been investigated.

OPEN ACCESS

Based on the above analyses, $\text{La}_{1-x}\text{Nd}_x\text{Co}_{0.3}\text{Fe}_{0.7}\text{O}_3$ could be very promising for the CO sensing; there must be an optimal x value for obtaining the best CO sensing performance. In this work, we prepared $\text{La}_{1-x}\text{Nd}_x\text{Co}_{0.3}\text{Fe}_{0.7}\text{O}_3$ nanoparticles by co-precipitation and investigated the CO sensing properties of the $\text{La}_{1-x}\text{Nd}_x\text{Co}_{0.3}\text{Fe}_{0.7}\text{O}_3$ system, with an aim to exploit the optimal chemical composition for the best CO sensing performances. It is discovered that the $\text{La}_{0.7}\text{Nd}_{0.3}\text{Co}_{0.3}\text{Fe}_{0.7}\text{O}_3$ sensor shows the best CO sensing performances.

2. Methods

A chemical co-precipitation method was used to prepare $\text{La}_{1-x}\text{Nd}_x\text{Co}_{0.3}\text{Fe}_{0.7}\text{O}_3$ nanoparticles ($x = 0 \div 1.0$ with increment 0.1). The stoichiometric amounts of corresponding metal nitrates were dissolved in deionized water. H_2O_2 was then added to oxidize Co(II) to Co(III). Afterwards, NaOH solution was added to adjust the pH value to 11~12. The resulted precipitate was rinsed with deionized water until pH=7, and dried at 80°C for 2 h. Finally, $\text{La}_{1-x}\text{Nd}_x\text{Co}_{0.3}\text{Fe}_{0.7}\text{O}_3$ nanoparticles were obtained by calcination at 650°C for 6 h in air.

The gas sensors were fabricated by dipping. The $\text{La}_{1-x}\text{Nd}_x\text{Co}_{0.3}\text{Fe}_{0.7}\text{O}_3$ nanoparticles were dispersed in ethanol ultrasonically. Then, the suspension was dripped on the FTO substrate, on which a gap of about 60 μm was cut by laser. Afterwards, the samples were dried naturally to remove ethanol. Platinum wire was connected to the FTO using Ag paste.

The crystal structure of the $\text{La}_{1-x}\text{Nd}_x\text{Co}_{0.3}\text{Fe}_{0.7}\text{O}_3$ powder was checked by X-ray diffraction (XRD) (SHIMADZU XRD-7000S) in the 2θ range of 10-90°. The microstructure of $\text{La}_{1-x}\text{Nd}_x\text{Co}_{0.3}\text{Fe}_{0.7}\text{O}_3$ sensors was analyzed using scanning electron microscopy (SEM) equipped with an energy dispersive X-ray spectroscope (EDS). The sensor resistance was collected automatically every second using a Keithley 2450 Source Measurement Unit (SMU). A flow system comprising two mass flow controllers was used to introduce gases with specified concentrations of CO in N_2 into the sample chamber at a flow rate of 500 standard centi-cubic per minute (SCCM).

3. Results

3.1. Phase determination and microstructure

Fig. 1 shows the XRD patterns of the $\text{La}_{1-x}\text{Nd}_x\text{Co}_{0.3}\text{Fe}_{0.7}\text{O}_3$ nanoparticles prepared by co-precipitation; all of them are single phase. The corresponding spectra of rhombohedral LaCoO_3 (orange line), orthorhombic LaFeO_3 (violet line), NdCoO_3 (red line), and NdFeO_3 (blue line) are reported for comparison. When $x = 0$, the $\text{LaCo}_{0.3}\text{Fe}_{0.7}\text{O}_3$ nanoparticles have the transient phases between LaCoO_3 and LaFeO_3 . When $x = 1$, the $\text{NdCo}_{0.3}\text{Fe}_{0.7}\text{O}_3$ nanoparticles have the transient phases between NdCoO_3 and NdFeO_3 . In addition, the angle of the Bragg reflections of the $\text{La}_{1-x}\text{Nd}_x\text{Co}_{0.3}\text{Fe}_{0.7}\text{O}_3$ nanoparticles increases with an increase of Nd content x . This is because the radius of the Nd^{3+} (98 pm) ion is smaller than that of La^{3+} (103 pm), when the La^{3+} is replaced by Nd^{3+} at A site,

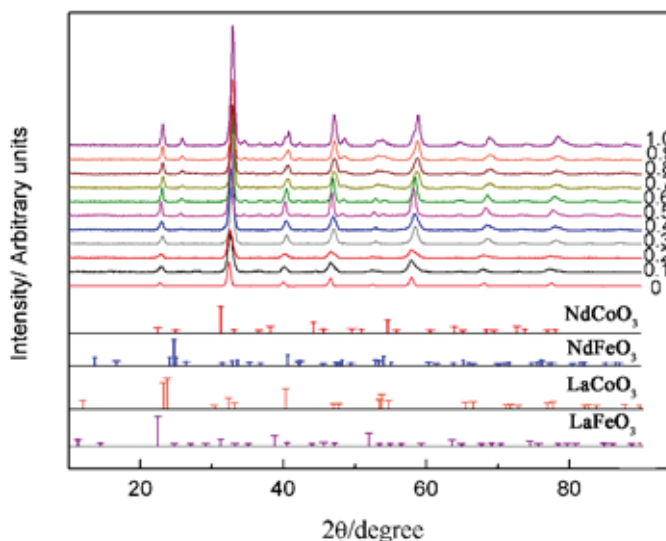


Figure 1: XRD patterns of $\text{La}_{1-x}\text{Nd}_x\text{Co}_{0.3}\text{Fe}_{0.7}\text{O}_3$ nanoparticles ($0 \leq x \leq 1$).

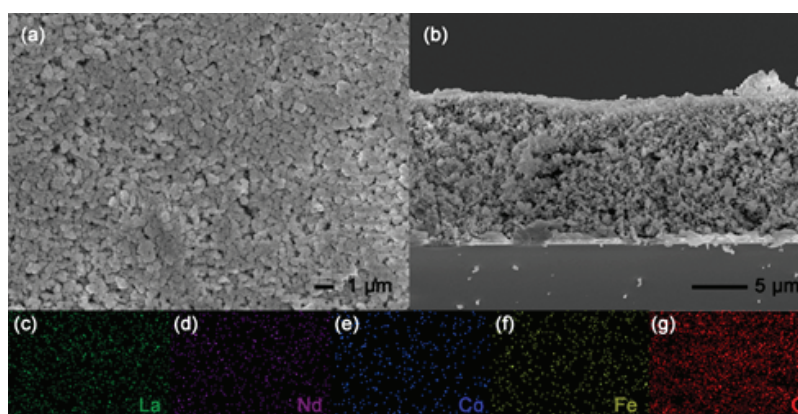


Figure 2: SEM micrographs of $\text{La}_{0.7}\text{Nd}_{0.3}\text{Co}_{0.3}\text{Fe}_{0.7}\text{O}_3$ sensor: (a) surface, (b) cross-section. EDS elemental mapping showing distribution of (c) La, (d) Nd, (e) Co, (f) Fe and (g) O elements in $\text{La}_{0.7}\text{Nd}_{0.3}\text{Co}_{0.3}\text{Fe}_{0.7}\text{O}_3$ sensor.

the lattice parameters should become smaller with increase of the Nd concentration. According to the Bragg formula, the diffraction angle becomes larger.

Typical SEM micrographs of the $\text{La}_{0.7}\text{Nd}_{0.3}\text{Co}_{0.3}\text{Fe}_{0.7}\text{O}_3$ sensor are shown in Fig. 2. From the Fig. 2a, we can see that the sensing layer is highly porous and the original morphology of particles is well maintained, which is preferred for gas-sensing applications. A clear boundary exists between the $\text{La}_{0.7}\text{Nd}_{0.3}\text{Co}_{0.3}\text{Fe}_{0.7}\text{O}_3$ layer and the FTO substrate, as indicated in Fig. 2g. Good adhesion between the sensing layer and the substrate is also obvious. The representative EDS elemental mappings of the $\text{La}_{0.7}\text{Nd}_{0.3}\text{Co}_{0.3}\text{Fe}_{0.7}\text{O}_3$ sensor are illustrated in Figs. 2c-g suggesting that the elements La, Nd, Co, and Fe show the homogeneous distribution throughout the sensor.

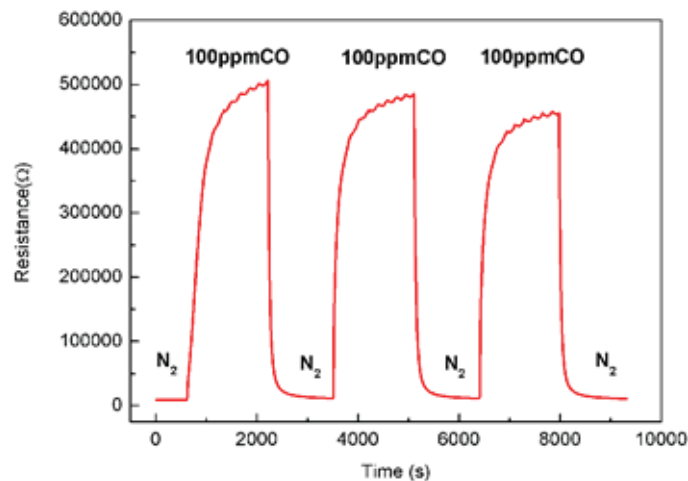


Figure 3: Resistance of $\text{La}_{0.7}\text{Nd}_{0.3}\text{Co}_{0.3}\text{Fe}_{0.7}\text{O}_3$ sensor under alternating cycles of 100 ppm CO and N_2 at 250°C .

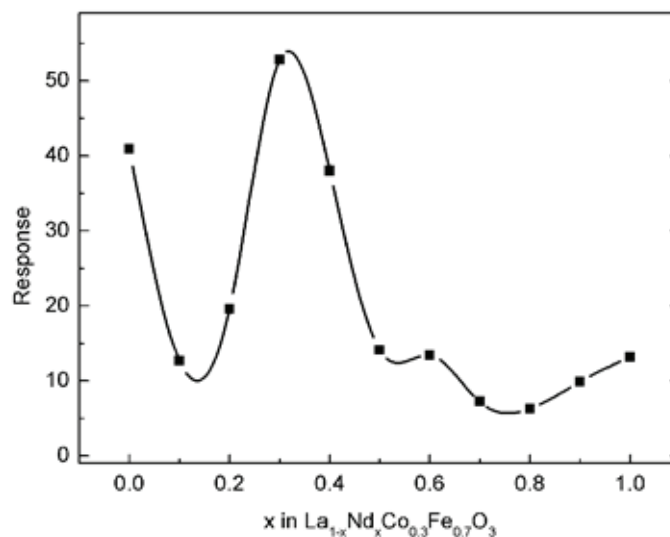


Figure 4: Response of $\text{La}_{1-x}\text{Nd}_x\text{Co}_{0.3}\text{Fe}_{0.7}\text{O}_3$ sensor as a function of x ($0 \leq x \leq 1$) for 100 ppm CO at 250°C .

3.2. Sensing Properties to CO

The resistance of $\text{La}_{1-x}\text{Nd}_x\text{Co}_{0.3}\text{Fe}_{0.7}\text{O}_3$ sensors ($x = 0 \div 1.0$ with increment 0.1) were tested under alternating cycles of 100 ppm CO and N_2 at 250°C ; the resistance curve of the $\text{La}_{0.7}\text{Nd}_{0.3}\text{Co}_{0.3}\text{Fe}_{0.7}\text{O}_3$ sensor under alternating cycles of 100 ppm CO and N_2 at 250°C is shown in Fig. 3. When 100 ppm CO was introduced, the sensor resistance increased, and a resistance decrease was observed when CO was cut off. A good repeatability was achieved among individual cycles. The sensor response is defined as: $S = R_{\text{CO}}/R_{\text{N}_2}$, here R_{CO} is the sensor resistance in the presence of CO, and R_{N_2} is the resistance in N_2 . It can be calculated from the resistance curve.

Fig. 4 shows the response of the $\text{La}_{1-x}\text{Nd}_x\text{Co}_{0.3}\text{Fe}_{0.7}\text{O}_3$ sensors as a function of x at 250°C . As one can see, the responses of the $\text{La}_{1-x}\text{Nd}_x\text{Co}_{0.3}\text{Fe}_{0.7}\text{O}_3$ sensors fluctuate with the change of x . Among them, when $x = 0.3$, the $\text{La}_{0.7}\text{Nd}_{0.3}\text{Co}_{0.3}\text{Fe}_{0.7}\text{O}_3$ sensor displays an excellent response ($S = 52.8$).

4. Conclusion

The CO sensing properties of $\text{La}_{1-x}\text{Nd}_x\text{Co}_{0.3}\text{Fe}_{0.7}\text{O}_3$ were systematically investigated as a function of Nd concentration. Among them, the $\text{La}_{0.7}\text{Nd}_{0.3}\text{Co}_{0.3}\text{Fe}_{0.7}\text{O}_3$ sensor showed excellent CO sensing performance. Therefore, $\text{La}_{0.7}\text{Nd}_{0.3}\text{Co}_{0.3}\text{Fe}_{0.7}\text{O}_3$ is a very promising material for the CO sensors.

5. Acknowledgement

This work is partly supported by the Graduates' Innovation and Entrepreneurship Foundation (0118650018), Huazhong University of Science and Technology.

References

- [1] A. V. Salker, N.-J. Choi, J.-H. Kwak, B.-S. Joo, and D.-D. Lee, Thick films of In, Bi and Pd metal oxides impregnated in LaCoO_3 perovskite as carbon monoxide sensor, *Sensors and Actuators, B: Chemical*, **106**, no. 1, 461–467, (2005).
- [2] T. Zhang, L. Liu, Q. Qi, S. Li, and G. Lu, Development of microstructure In/Pd-doped SnO_2 sensor for low-level CO detection, *Sensors and Actuators, B: Chemical*, **139**, no. 2, 287–291, (2009).
- [3] H. J. Jung, J.-T. Lim, S. H. Lee, Y.-R. Kim, and J.-G. Choi, Kinetics and mechanisms of CO oxidation on $\text{Nd}_{1-x}\text{Sr}_x\text{CoO}_{3-y}$ catalysts with static and flow methods, *Journal of Physical Chemistry*, **100**, no. 24, 10243–10248, (1996).
- [4] DH. Kim and Kim. , KH: Kinetics and oxygen vacancy mechanism of the oxidation of carbon-monoxide on perovskite $\text{Nd}_{1-x}\text{Sr}_x\text{CoO}_{3-y}$ solutions as a catalysis. Bull Kor Chem Soc, in *Kim KH: Kinetics and oxygen vacancy mechanism of the oxidation of carbon-monoxide on perovskite $\text{Nd}_{1-x}\text{Sr}_x\text{CoO}_{3-y}$ solutions as a catalysis*. Bull Kor Chem Soc, **15**, 616–622, 616–622, 15, 1994.
- [5] L. Malavasi, C. Tealdi, G. Flor, G. Chiodelli, V. Cervetto, A. Montenero, and M. Borella, NdCoO_3 perovskite as possible candidate for CO-sensors: Thin films synthesis and sensing properties, *Sensors and Actuators, B: Chemical*, **105**, no. 2, 407–411, (2005).
- [6] R. Zhang, J. Hu, Z. Han, M. Zhao, Z. Wu, Y. Zhang, and H. Qin, Electrical and CO-sensing properties of $\text{NdFe}_{1-x}\text{Co}_x\text{O}_3$ perovskite system, *Journal of Rare Earths*, **28**, no. 4, 591–595, (2010).
- [7] N. T. Thuy, D. L. Minh, H. T. Giang, and N. N. Toan, Structural, electrical, and ethanol-sensing properties of $\text{La}_{1-x}\text{Nd}_x\text{FeO}_3$ nanoparticles, *Advances in Materials Science and Engineering*, **2014**, Article ID 685715, (2014).